Acoustically shaped laser light as an enabling technology for Industry 4.0

Salvatore Surdo[1,*], Alessandro Zunino[1,2], Alberto Diaspro[1], Marti Duocastella[1]

[1]Nanophysics, Istituto Italiano di Tecnologia, via Morego 30, 16123 Genova, Italia
[2]Physics Department, University of Genoa, Via Dodecaneso 33, 16146, Genova, Italy
mail: salvatore.surdo@iit.it, marti.duocastella@iit.it

***Abstract*— The wide material options and functionalities of direct laser writing (LDW) systems make them ideal candidates as digital manufacturing tools of Industry 4.0. However, the inherent serial nature of LDW can heavily limit processing throughput and the participation of lasers to the fourth industrial revolution. Here we present a novel acusto-optofluidic (AOF) system that boosts speed and design flexibility of LDW. The AOF employs acoustic standing waves in a liquid to produce complex light intensity patterns at sub-microsecond temporal resolution. By varying the driving parameters such as frequency, amplitude, and phase of the acoustic waves, we demonstrate large-area (cm^2) additive as well as subtractive direct manufacturing of user-selectable patterns with nanometric spatial resolution. The AOF-enabled laser workstation can be digitally controlled and cloudily interconnected, opening the door to the application of lasers to smart-factories with high level of operational flexibility, productivity, and automatization.**

Keywords*— direct-write, high-throughput, laser processing, Internet of things, cyber systems

I. Introduction

The term Industry 4.0 denotes the so-called fourth industrial revolution that is currently driven by Internet-derived technologies or Internet of Things (IoT) as vehicles for synergistically interconnecting humans with machines [1], [2]. This industrial model holds the promise of high flexibility in manufacturing, massive customization, and enhanced productivity. The paradigm of Industry 4.0 demands for technologies capable of integrating data exchange with automation in order to monitor physical processes and make decentralized decisions.

So far, several methods exist for rapid data acquisition, exchange, and analysis. Key examples include sensors (e.g. cameras, thermometers) that allow monitoring of physical processes in real time [3], and communication technologies (e.g. radio frequency identification or RFID) that enable direct interaction between various manufacturing tools [4]. Combined with advanced algorithms (e.g. machine learning), these systems allow adaptive decisions to be made in a timely fashion. However, a central problem still remains unsolved in the paradigm of Industry 4.0, namely the selection of the ideal tool for machining the workpiece in these digitally interconnected systems.

The perfect candidate for this task should offer high speed and large flexibility in terms of material options, patterns selection, and functionalities. Laser direct-writing (LDW) systems fulfill all these conditions. Indeed, lasers can process an extremely wide range of materials including metals, plastics, ceramics, glass, and even biological matter [5]–[7]. Furthermore, lasers can operate in either additive or subtractive modes thus enabling material deposition as well as ablation and, hence, drilling, cutting, joining of various materials or roughening, smoothing, coating, patterning, and cleaning of target surfaces [8]–[10]. Importantly, lasers can be controlled numerically and, hence, easily connected with other digitally coordinated systems or machines.

Despite their great potential, lasers are still at the margins of Industry 4.0, mainly because of their inherent serial nature – in a typical LDW system the laser beam moves point-by-point respect to the workpiece – that heavily limits the throughput of current laser-based machining tools. A myriad of approaches have been developed to enhance both speed and pattern flexibility of conventional LDW systems. Regardless of the specific solution, the fundamental strategy has been shifting the operational principle of LDW from single-point to area processing.

LDW parallelization is typically achieved by shaping the intensity of the laser beam to a customized pattern. Beam shaping methods can be as simple as a fixed optical element (e.g. a binary mask or a diffractive optical element) and a projection lens, but these systems inevitably sacrifice flexibility in pattern selection [11], [12]. This has spurred the development of more complex architectures that offer dynamic and rapid beam shaping, such as digital micromirror devices (DMDs) and spatial light modulators (SLMs) [13], [14]. Even if high throughput laser manufacturing has been proven with these devices, they can suffer from limited modulation depth, poor diffraction efficiency, complex setups, low damage thresholds, low refresh rate (from 10 Hz to 200 Hz) or high cost.

In this work, we present an original acusto-optofluidics (AOF) approach for laser-beam shaping at unprecedented rates, with high efficiency, no pixelation effects, ease of implementation and low cost. Our method exploits acoustic waves in a liquid for the rapid generation and selection of laser-interference patterns [15]. The integration of the AOF system into a LDW station enables high-throughput laser direct manufacturing of user-selectable patterns over indeterminately large areas and of various materials.

Here, we describe the operational principle behind the AOF technology and present an in-depth experimental characterization of the system. We also show its feasibility for Industry 4.0 by using it as an additive and subtractive manufacturing tool.

978-1-7281-0429-4/19/$31.00 ©2019 IEEE

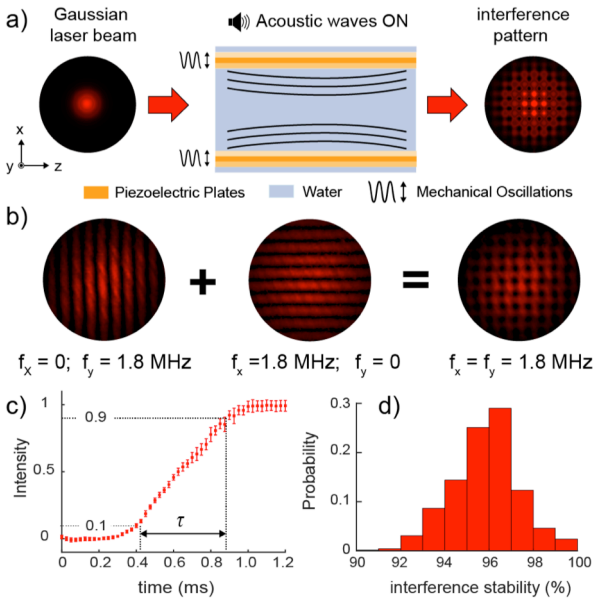

Figure 1. Light shaping with acusto-optofluidics. a) Schematics of the acusto-optofluidic cavity. For simplicity only one couple of piezoelectric plates is represented. Mechanical oscillations of the plates alter the water refractive index. Simulations show how the interaction of a Gaussian laser-beam travelling through the cavity with the acoustically controlled refractive index profile leads to interference at the output of the AOF cavity. b) Examples of intensity patterns generated with a 647 nm continuous-wave (CW) laser and different driving conditions of the cavity. c) Response time of the cavity and d) distribution of the autocorrelation coefficients of the acoustically generated pattern over an interrogational window as large as two hours.

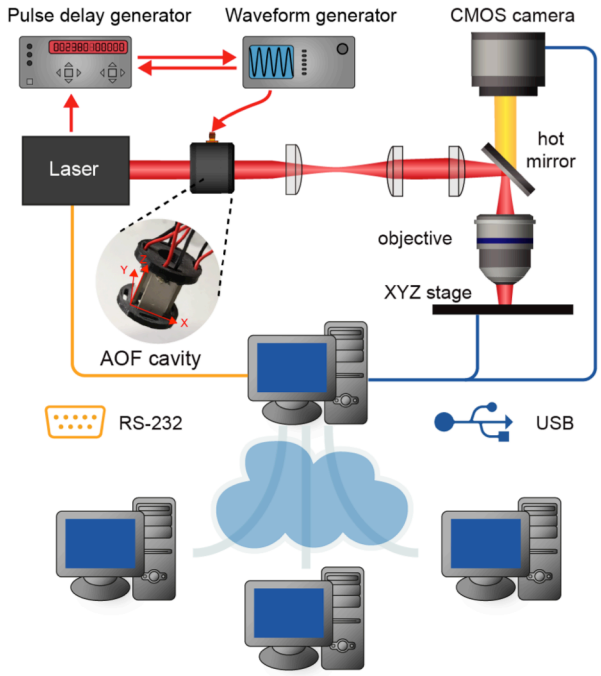

Figure 2. Schematic of the main components of the acusto-opto-fluidic laser direct-write system. The AOF cavity is conjugated with the plane of the workpiece through a 4f-system (f1=250mm,f2=150mm in our experiments), which magnifies/de-magnifies the intensity pattern thus providing an additional degree of tunability to our method. The AOF-LDW system can be connected to other workstations or IoT-nodes through an IoT-network. The network provides Internet connectivity to the entire LDW station, collects images recorded by the CMOS camera, and send data (e.g. CAD files of either the intensity pattern or the workpiece being generated) to the AOF system, the laser, and the XYZ stage

II. OPERATIONAL PRINCIPLE AND CHARACTERIZATION OF THE ACUSTO-OPTOFLUIDIC SYSTEM

The core component of the AOF-LDW system is an acoustic resonant cavity immersed in a liquid transparent to the laser radiation [15]. The cavity consists of two pairs of piezoelectric rectangular plates oriented along two orthogonal directions, namely *X*- and *Y*-axis. By driving each piezoelectric pair with sinusoidal signals, acoustic waves are generated in the fluid (water in current experiments). On resonance, these waves cause a periodic modulation in the density and, hence, in the refractive index of the liquid. As shown in Figure 1a, the interaction of a laser beam propagating through the cavity (in the *Z* direction) with this acoustically altered medium produces light intensity patterns. Importantly, by adjusting the technological parameters such as frequency and amplitude of the driving signals, various customized patterns can be easily generated. Figure 1b shows some examples of the intensity patterns that are feasible with our method. In particular, one-dimensional (1D) patterns oriented along the *X*- or *Y*-axis as well as two-dimensional (2D) light intensity distributions were generated by driving one or both piezoelectric couples at the resonant frequency of 1.8 MHz.

Reliability and speed are important parameters of any machining tools suitable for Industry 4.0 [16], [17], since they enable high-quality production, quick customization, and short time-to-market responses. With this in mind, we characterized the performance of the AOF system in terms of temporal response and pattern stability. The former was calculated as the time needed for an acoustically generated intensity pattern to rise from 10% to 90% of its steady-state value. Pattern stability, on the other hand, was calculated as the correlation coefficient between a series of images of an intensity pattern and a reference image acquired at t = 0 s. Interestingly, we found that the AOF system reaches steady-state in lower than 500 μs (Figure 1c) and the generated pattern remained stable within a large temporal interval of 2 hours with an average interference stability of about 96% (Figure 1d). Importantly, at the steady-state, the use of pulsed lasers synchronized with the driving signals allows light interacting with an instantaneous refractive index profile and, hence, intensity pattern selection at sub-microsecond timescales [15].

III. LASER MATERIAL PROCESSING WITH THE ACUSTO-OPTO-FLUIDIC SYSTEM

To demonstrate the feasibility of our approach as a manufacturing tool we integrated the AOF system into a LDW station. As depicted in Figure 2, the AOF-enabled workstation consists of a pulsed femtosecond laser (pulse-width 70 fs at λ = 800 nm), an up-right microscope with a long-working distance objective (50×/0.55 NA), and an XYZ stage. Waveform and pulse delay generators are used for driving the AOF cavity. A CMOS camera is coaxially coupled to the microscope objective for real-time workpiece inspection. Importantly, this option can be also used for sample tagging and/or identification within the entire manufacturing chain.

The setup is controlled with a LabView program running on a computer that is connected to Internet and to other computers or tools, allowing IoT-enabled manufacturing. More in details, this option can be used for data storage or exchange as well as software updating, remote process control and monitoring. The AOF-LDW station can therefore

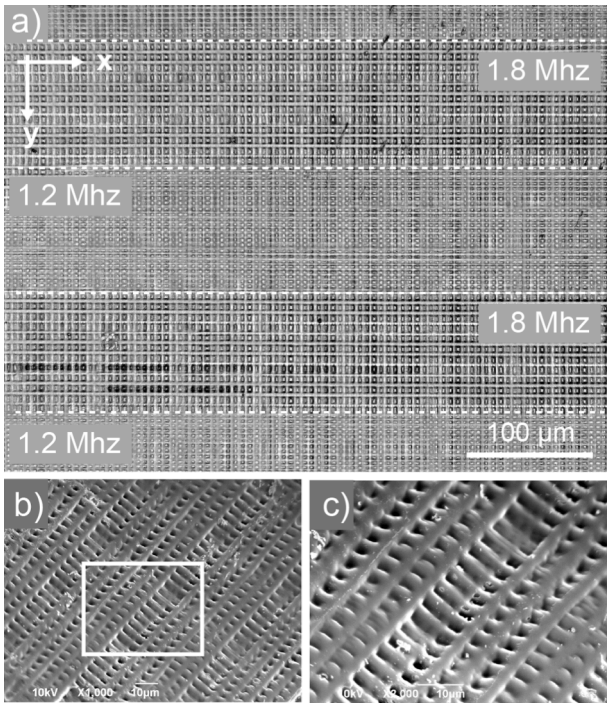

Figure 3. Additive-manufacturing with the AOF-LDW station. a) Optical image of polymeric regular structures obtained by snake scanning in X and Y an 800 nm pulsed laser at 0.3 mm/s. Along the X-axis the acoustic frequency was 1.2 MHz whereas along the Y -axis the acoustic frequency was binary modulated between 1.2 MHz and 1.8 MHz. c-d) Scanning electron micrographs (SEM) of a magnified portion of the polymeric structures shown in (a).

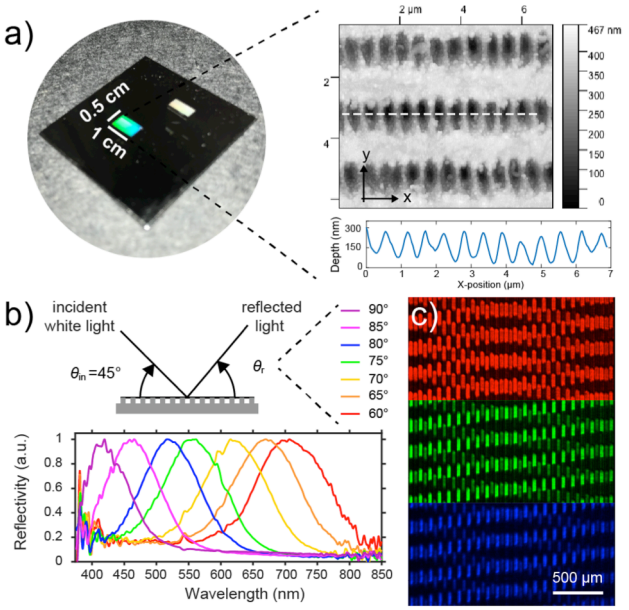

Figure 4. Subtractive-manufacturing with the AOF-LDW station. a) Optical image of a large-area (~cm^2) ablated on palladium with acoustically shaped laser light. Atomic force microscopy (AFM) on a portion of the generated pattern reveals the presence of periodically arranged nanostructures on the laser-treated regions. b) Angle resolved reflectivity measurements on the sample shown in (a). For an incident angle of 45° the ablated structures scatter the incoming white light with angles from 60° to 90° for wavelengths between 400 and 800 nm. c) Array of structurally colored micro-pixels obtained by modulating the acoustic frequency at various rates. Depending in the incident angle red, green and blue pixels are clearly visible.

use IoT technologies to create or access to a virtual copy of both the product being manufactured and the manufacturing environment, monitor the fabrication processes, and eventually adapt or reconfigure it on the basis of fidelity between the real product and its digital avatar. Importantly, the high speed in the pattern selection of the AOF system allows these operations to be quickly performed, thus enabling the implementation of cyber machining tools that can vary, correct, and optimize their behaviors in a timely fashion.

The functionalities of the AOF-LDW system for Industry 4.0 were tested in both additive and subtractive modes. Figure 3 shows some representative examples of photo-polymerized structures formed with the proposed AOF-LDW workstation. In this experiment, an epoxy resin was scanned, first along the *X*-axis with an intensity pattern generated at the acoustic frequency of 1.2 MHz, and then along the *Y*-axis while the acoustic frequency was binary switching between 1.2 MHz and 1.8 MHz. The effect of this modulation on the topology of the structure is clearly visible in Figure 3a, whereas the scanning electron micrographs of Figure 3b and 3c well highlight the high quality of the resulting surfaces.

Figure 4 shows examples of large-area (~cm^2) patterns obtained by laser-ablation of a palladium substrate. In this experiment, the sample surface was snake-scanned with an intensity pattern generated at the acoustic frequency of 1.6 MHz. This strategy resulted in periodic microstructures (period of ~ 2 µm) aligned with the interference (i.e., scan direction) and integrating periodic nanostructures (period of about 600 nm) orthogonal to the scan direction. Interestingly, the generated structures are already functional since they enable structural coloration of the substrate as shown in the optical image of Figure 4a. In particular, angle-resolved reflectivity measurements proved that the generated pattern reflects the entire gamma of wavelengths in the visible (Figure 4b). We exploited this feature for integrating into a palladium substrate a large (~0.5×1 cm^2) array of structurally colored pixels with different sizes (Figure 4c). This result corroborates the suitability of the AOF-LDW system for important industrial applications including, photonics, displays, decoration of consumer products (e.g. food, jewels, and fashion items), tagging and anti-counterfeiting [18]-[22].

IV. CONCLUSION

We demonstrated feasibility and functionality of an acusto-optofluidic system for the rapid generation of user-selectable light intensity patterns. In particular, the topology of the pattern depends on the amplitude, frequency, and phase of the acoustic waves and, hence, pattern control is possible by adjusting the driving signals. As our results demonstrate, the AOF system can be easily integrated into a LDW station and enables high-throughput processing of various materials in both additive and subtractive modes. Importantly, the AOF-LDW station is digitally controlled and can be connected to other IoT technologies enabling delocalized and rapid control of the manufacturing chain.

By combining the high throughput and flexibility of the acusto-optofluidic system with the large functionality options of IoT-derived technologies, the AOF-LDW station represents a credible candidate as machining tool of Industry 4.0. Here, we can anticipate that in conjunction with the use of artificial intelligence or machine learning, the AOF-LDW system will enable the implementation of autonomous IoT-based manufacturing tools that adapt their action in response to external stimuli, recorded data, or learning abilities.

V. MATERIALS AND METHODS

AOF system implementation: The acoustic cavity of this work consists of two couples of parallel and rectangular piezoelectric plates. The plates were mounted on 3D-printed supports designed so that each couple resulted orthogonal to the other. Once assembled, the AOF cavity was placed in a metallic black cylinder. O-rings and epoxy resin were used to seal the cylinder with two circular windows featuring an optical transmission of 93.8% in the wavelength interval 185 nm – 2.1 μm. Four holes were drilled onto the cylinder and used to mount electrical connectors and fluidic ports. Specifically, two coaxial RF connectors (SMA–50Ω, RS Components) were glued to the cylinder with epoxy resin and used to provide driving signals to each plate couple. Similarly, two Luer-lock connectors were used as inlet and outlet ports for filling the cylinder and, hence, the cavity with Mili-Q water. Two arbitrary and independent waveform generators (GFG2004, ISO-TECH) with a maximum peak-to-peak voltage of 20 V were used to drive the AOF system.

Optical simulations: Theoretical acoustically generated laser interference patterns were calculated by solving the Fresnel diffraction integral using Matlab. The main input parameters of the model were the rheological and optical properties of the liquid, the geometrical parameters of the cavity, and the wavelength and beam size of the incoming laser [15].

AOF cavity optical characterization: A 647-nm CW laser (OBIS LX, Coherent) was expanded, collimated, and finally directed towards the AOF cavity. Two adjustable mirrors were used to ensure that the beam was coaxially coupled with the cylinder. The exit plane of the AOF cavity was conjugated with the back-focal plane of a telescope with a magnification of 0.6. The interference patterns generated after the telescope were then recorded with a CMOS camera (DCC1545M, Thorlabs).

Material processing: The AOF-LDW consists of modelocked Ti:sapphire laser (Micra, Coherent) optically pumped by CW green laser (Verdi, Coherent), a microscope objective (Mitutoyo MPlan-Apo, 50×/0.55NA), an up-right microscope, and the AOF cavity, which was conjugated to the sample plane by means of relay lenses. The laser emits 70-fs pules (energy per pulse up to 2.5 mJ/cm^2) at λ=800 nm with a repetition rate of 1 kHz. A rotating half-wave plate in conjunction with a polarizing beam splitter allowed a fine control of the beam-energy. The sample being irradiated was moved relative to the interference pattern by using a XYZ stage (Prior Scientific) with a spatial resolution <10 nm, a translation speed as high as 6 mm/s, and a travel range of 11.2 cm × 11.2 cm × 0.73 cm.

Periodic lines were ablated by moving the substrate with respect to the interference pattern (average energy per pulse ~4.2 μJ) at a scan-speed of 0.15 mm·s^{-1}. For two-photon polymerization experiments, a negative photoresist, namely a mixture (0.08%) of Pentaerythritol triacrylate (Sigma) and isopropylthioxanthone (Sigma), was squeezed between two glass-cover slips mounted on the XYZ stage of the LDW. After irradiation with the interference pattern (energy per pulse 0.3 μJ), the resist was immersed in methanol for 5 min and rinsed with isopropanol to remove the monomer.

Samples Characterization: Morphology of the laser-irradiated samples was investigated with scanning electron microscopy (JSM-6390, JEOL) at an acceleration voltage of 10 kV. In order to inhibit charging effects, polymeric samples were sputter-coated with 10-nm of gold. 3D height maps of the laser-formed pixels were acquired with an atomic force microscope (MFP-3D, Asylum Research) operating in tapping mode. The probes used were Al-coated Si cantilevers (Nanosensors) with a nominal resonance frequency of 330 kHz, a spring constant of 40 N/m, and a tip-radius 5 nm. Images (amplitude data) were collected by scanning regions with an area of 7 μm × 7 μm at a resolution of 256 × 256 pixel.

Laser-induced structural colorations were experimentally characterized by means of scatterometry. Specifically, a fiber-coupled photo-spectrometer (Avantes) was used to record the pixel reflectivity in the wavelength interval 350-850 nm. The readout fiber was mounted on a rotating stage (RP01, Thorlabs) in order to collect diffracted light at various angles, namely from 60° to 90°. A low numerical aperture converging lens was used for shading the light of a white LED against the sample surface with an incident angle of 45°. The recorded reflectivity spectra were normalized respects their maximum.

REFERENCES

[1] R. Y. Zhong, X. Xu, E. Klotz, and S. T. Newman, "Intelligent Manufacturing in the Context of Industry 4.0: A Review," Engineering, vol. 3, no. 5, pp. 616–630, 2017.

[2] P. Daponte, F. Lamonaca, F. Picariello, L. De Vito, G. Mazzilli, and I. Tudosa, "A Survey of Measurement Applications Based on IoT," 2018 Workshop on Metrology for Industry 4.0 and IoT, MetroInd 4.0 and IoT 2018 - Proceedings, no. i, pp. 157–162, 2018.

[3] L. Gallucci, C. Menna, L. Angrisani, D. Asprone, R. S. Lo Moriello, F. Bonavolontá, and F. Fabbrocino, "An embedded wireless sensor network with wireless power transmission capability for the structural health monitoring of reinforced concrete structures," Sensors, vol. 17, no. 11, 2017.

[4] M. A. Tahir, B. Ramis Ferrer, and J. L. Martinez Lastra, "An Approach for Managing Manufacturing Assets through Radio Frequency Energy Harvesting," Sensors, vol. 19, no. 3, 2019.

[5] S. Surdo, S. Piazza, A. Diaspro, L. Ceseracciu, and M. Duocastella, "Towards nanopatterning by femtosecond laser ablation of pre-stretched elastomers," Applied Surface Science, vol. 374, pp. 151–156, 2015.

[6] H. Lin, H. Wang, X. Hu, L. Zheng, and C. Wang, "Laser drilling of structural ceramics A review," Journal of the European Ceramic Society, vol. 37, no. 4, pp. 1157–1173, 2016.

[7] P. Serra, D. Zafra, J. Morenza, M. Duocastella, and J. Fernández-Pradas, "Novel laser printing technique for miniaturized biosensors preparation," Sensors and Actuators B: Chemical, vol. 145, no. 1, pp. 596–600, 2009.

[8] C. B. Arnold, P. Serra, and A. Piqué, "Laser Direct-Write Techniques for Printing of Complex Materials," MRS Bulletin, vol. 32, no. 01, pp. 23–32, 2011.

[9] S. Surdo, R. Carzino, A. Diaspro, and M. Duocastella, "Single-Shot Laser Additive Manufacturing of High Fill-Factor Microlens Arrays," Advanced Optical Materials, vol. 6, no. 5, 2018.

[10] S. Surdo, A. Diaspro, and M. Duocastella, "Microlens fabrication by replica molding of frozen laser-printed droplets," Applied Surface Science, vol. 418, pp. 554–558, 2017.

[11] F. Brandi, N. Burdet, R. Carzino, and A. Diaspro, "Very large spot size effect in nanosecond laser drilling efficiency of silicon." Optics express, vol. 18, no. 22, pp. 23 488–94, 2010.

[12] L. Kelemen, S. Valkai, and P. Ormos, "Parallel photopolymerisation with complex light patterns generated by diffractive optical elements," Optics Express, vol. 15, no. 22, p. 14488, 2007.

[13] R. C. Y. Auyeung, H. Kim, S. Mathews, and A. Piqué, "Laser forward transfer using structured light," Optics Express, vol. 23, no. 1, p. 422, 2015.

[14] S. Behera, M. Kumar, and J. Joseph, "Submicrometer photonic structure fabrication by phase spatial-light-modulator-based interference lithography," Optics Letters, vol. 41, no. 8, p. 1893, 2016.

[15] S. Surdo and M. Duocastella, "Fast Acoustic Light Sculpting for Ondemand Maskless Lithography," Advanced Science, 2019, DOI:10.1002/advs.201900304.

[16] X. Xu, "Machine Tool 4.0 for the new era of manufacturing," International Journal of Advanced Manufacturing Technology, vol. 92, no. 5-8, pp. 1893–1900, 2017.

[17] G. Barillaro, S. Merlo, S. Surdo, L. M. Strambini, and F. Carpignano, "Optical quality-assessment of high-order one-dimensional silicon photonic crystals with a reflectivity notch at λ~1.55 μm," IEEE Photonics Journal, vol. 2, no. 6, pp. 981–990, 2010.

[18] S. Surdo, F. Carpignano, G. Silva, S. Merlo, and G. Barillaro, "An all-silicon optical platform based on linear array of vertical high aspect-ratio silicon/air photonic crystals," Appl. Phys. Lett., vol. 103, p. 171103, 2013.

[19] A. C. Arsenault, D. P. Puzzo, I. Manners, and G. A. Ozin, "Photonic-crystal full-colour displays," Nat. Photonics, vol. 1, no. 8, pp. 468–472, 2007.

[20] G. Polito, V. Robbiano, C. Cozzi, F. Cacialli, and G. Barillaro, "Template-Assisted Preparation of Micrometric Suspended Membrane Lattices of Photoluminescent and Non-Photoluminescent Polymers by Capillarity-Driven Solvent Evaporation: Application to Microtagging," Sci. Rep., vol. 7, no. 1, pp. 1–11, 2017.

[21] H. Hu, Q. W. Chen, J. Tang, X. Y. Hu, and X. H. Zhou, "Photonic anti-counterfeiting using structural colors derived from magnetic-responsive photonic crystals with double photonic bandgap heterostructures," J. Mater. Chem., vol. 22, no. 22, pp. 11048–11053, 2012.

[22] C. Y. Peng et al., "Flexible Photonic Crystal Material for Multiple Anticounterfeiting Applications," ACS Appl. Mater. Interfaces, vol. 10, no. 11, pp. 9858–9864, 2018.